

SUMO-interacting motif also enhances binding affinity (24), similar to LIR modification. Notably, a number of known autophagy receptors contain conserved serine residues adjacent to their LIRs, including NIX and NBR1, indicating a potentially broader impact of phosphorylation of autophagy processes. Interestingly, LC3A and LC3B have phosphorylated serine/threonine residues in their N-terminal extensions that are crucial for the interaction with LIR motifs (25, 26). Taken together, phosphorylation of ubiquitin-like modifiers and their binding domains brings another layer of complexity in controlling ubiquitin and autophagy signaling networks (27).

References and Notes

- H. Nakatogawa, K. Suzuki, Y. Kamada, Y. Ohsumi, *Nat. Rev. Mol. Cell Biol.* **10**, 458 (2009).
- Z. Yang, D. J. Klionsky, *Curr. Opin. Cell Biol.* **22**, 124 (2010).
- B. Levine, N. Mizushima, H. W. Virgin, *Nature* **469**, 323 (2011).
- V. Deretic, *Curr. Opin. Cell Biol.* **22**, 252 (2010).
- V. Kirkin, D. G. McEwan, I. Novak, I. Dikic, *Mol. Cell* **34**, 259 (2009).
- C. Kraft, M. Peter, K. Hofmann, *Nat. Cell Biol.* **12**, 836 (2010).
- D. G. McEwan, I. Dikic, *Trends Cell Biol.* **21**, 195 (2011).
- I. Novak *et al.*, *EMBO Rep.* **11**, 45 (2010).
- V. Kirkin *et al.*, *Mol. Cell* **33**, 505 (2009).

- Materials and methods are available as supporting material on *Science* Online.
- S. Pankiv *et al.*, *J. Biol. Chem.* **282**, 24131 (2007).
- C. Behrends, M. E. Sowa, S. P. Gygi, J. W. Harper, *Nature* **466**, 68 (2010).
- Single-letter abbreviations for the amino acid residues are as follows: A, Ala; D, Asp; E, Glu; F, Phe; G, Gly; I, Ile; and S, Ser.
- S. Wagner *et al.*, *Oncogene* **27**, 3739 (2008).
- S. Morton, L. Hesson, M. Pegg, P. Cohen, *FEBS Lett.* **582**, 997 (2008).
- K. Clark, L. Plater, M. Pegg, P. Cohen, *J. Biol. Chem.* **284**, 14136 (2009).
- A. L. Radtke, L. M. Delbridge, S. Balachandran, G. N. Barber, M. X. O'Riordan, *PLoS Pathog.* **3**, e29 (2007).
- T. L. Thurston, G. Ryzhakov, S. Bloor, N. von Muhlinen, F. Randow, *Nat. Immunol.* **10**, 1215 (2009).
- L. A. Knodler *et al.*, *Proc. Natl. Acad. Sci. U.S.A.* **107**, 17733 (2010).
- A. J. Perrin, X. Jiang, C. L. Birmingham, N. S. So, J. H. Brumell, *Curr. Biol.* **14**, 806 (2004).
- C. R. Beuzón *et al.*, *EMBO J.* **19**, 3235 (2000).
- Y. T. Zheng *et al.*, *J. Immunol.* **183**, 5909 (2009).
- M. Cemina, P. K. Kim, J. H. Brumell, *Autophagy* **7**, 341 (2011).
- P. Stehmeier, S. Muller, *Mol. Cell* **33**, 400 (2009).
- H. Jiang, D. Cheng, W. Liu, J. Peng, J. Feng, *Biochem. Biophys. Res. Commun.* **395**, 471 (2010).
- S. J. Cherra 3rd *et al.*, *J. Cell Biol.* **190**, 533 (2010).
- F. Ikeda, N. Crosetto, I. Dikic, *Cell* **143**, 677 (2010).

Acknowledgments: We thank P. Cohen, S. Mueller, K. Rajalingam, C. Behrends, and the members of

Dikic laboratory for constructive comments and critical reading of the manuscript; P. Cohen for OPTN and TBK1 reagents; and V. Kirkin for the initial yeast two-hybrid screens. This work was supported by grants from Deutsche Forschungsgemeinschaft, the Cluster of Excellence "Macromolecular Complexes" of the Goethe University Frankfurt (EXC115), the Landes-Offensive zur Entwicklung Wissenschaftlich-ökonomischer Exzellenz-fundiert Onkogene Signaltransduktion Frankfurt network, and the European Research Council (ERC) under the European Union's Seventh Framework Programme (FP7/2007-2013)/ERC grant agreement no. (250241-LineUb) to I.D. and partly by Swiss National Fonds (3100A0-121834/1) to D.B. The Center for Protein Research is funded by a generous grant from the Novo Nordisk Foundation. J.K. is supported by a scholarship from the Split, Croatia, government, S.W. by a postdoctoral fellowship from the Danish Council for Independent Research (F55: 10-085134), N.R.B. by the Initiative and Networking Fund of the Helmholtz Association, and H.F. by Swiss National Science Foundation (31003A-121834).

Supporting Online Material

www.sciencemag.org/cgi/content/full/science.1205405/DC1
Materials and Methods

Figs. S1 to S9

Table 1

References

10 March 2011; accepted 17 May 2011

Published online 26 May 2011;

10.1126/science.1205405

Adipose Triglyceride Lipase Contributes to Cancer-Associated Cachexia

Suman K. Das,¹ Sandra Eder,² Silvia Schauer,¹ Clemens Diwoy,³ Hannes Temmel,¹ Barbara Guertl,¹ Gregor Gorkiewicz,¹ Kuppusamy P. Tamilarasan,¹ Pooja Kumari,^{1,4} Michael Trauner,⁴ Robert Zimmermann,² Paul Vesely,¹ Guenter Haemmerle,² Rudolf Zechner,^{2*} Gerald Hoefler^{1*}

Cachexia is a multifactorial wasting syndrome most common in patients with cancer that is characterized by the uncontrolled loss of adipose and muscle mass. We show that the inhibition of lipolysis through genetic ablation of adipose triglyceride lipase (*Atgl*) or hormone-sensitive lipase (*Hsl*) ameliorates certain features of cancer-associated cachexia (CAC). In wild-type C57BL/6 mice, the injection of Lewis lung carcinoma or B16 melanoma cells causes tumor growth, loss of white adipose tissue (WAT), and a marked reduction of gastrocnemius muscle. In contrast, *Atgl*-deficient mice with tumors resisted increased WAT lipolysis, myocyte apoptosis, and proteasomal muscle degradation and maintained normal adipose and gastrocnemius muscle mass. *Hsl*-deficient mice with tumors were also protected although to a lesser degree. Thus, functional lipolysis is essential in the pathogenesis of CAC. Pharmacological inhibition of metabolic lipases may help prevent cachexia.

Cachexia (*kakos hexis*, Greek for "bad condition") is a devastating syndrome that frequently occurs in patients suffering from chronic infection, such as tuberculosis or AIDS,

and other diseases, including chronic obstructive pulmonary disease, chronic kidney disease, and chronic heart failure. Most commonly, however, cachexia is observed in cancer. The highest frequency of cancer-associated cachexia (CAC) occurs in pancreatic and gastric cancer (1–3). CAC is an important adverse prognostic factor and the immediate cause of death in an estimated 15% of all cancer patients (3–5). Wasting results from depletion of both adipose tissue and skeletal muscle (6, 7). In contrast to starvation, the non-muscle protein compartment of the body is relatively unaffected in CAC patients (7), implying a

tumor-associated metabolic condition that specifically targets adipose tissue and muscle. Thus, anorexia is unlikely to be solely responsible for the loss of skeletal muscle in patients with CAC. Indeed, nutritional supplementation has largely failed to reverse the wasting process (8).

The pathogenesis of CAC is multifactorial (9). Central mechanisms regulate appetite, food intake, and energy consumption. Contributing peripheral mechanisms control lipid and carbohydrate metabolism in various tissues. Severe lipid loss in CAC is driven by changes in lipid catabolism (10–15) and, possibly, lipogenesis (16). The concept that increased triacylglycerol (TG) degradation may contribute decisively to CAC is strongly underscored by increased plasma levels of fatty acids (FAs) and glycerol; increased lipolytic rates upon epinephrine stimulation; and increased expression of lipid-mobilizing factors, such as zinc- α 2 glycoprotein-1 (AZGP1), tumor necrosis factor α (TNF- α), and interleukins (IL)-1 and -6 (17, 18). The breakdown of fat requires lipolysis of TG stored in cellular lipid droplets and is mediated by adipose triglyceride lipase (ATGL) and hormone-sensitive lipase (HSL) (19). This led to our hypothesis that disruption of fat catabolism may prevent the initiation and/or progression of CAC. In vertebrates, lipolysis is most active in adipose tissue, with ATGL predominantly responsible for the initial step of TG hydrolysis (formation of diacylglycerol) and HSL for the hydrolysis of diacylglycerol. We investigated whether one or both of these lipases are essential for CAC.

To assess the role of lipases in CAC, we used two different cachexia models in mice lacking

¹Institute of Pathology, Medical University of Graz, 8036 Graz, Austria. ²Institute of Molecular Biosciences, University of Graz, 8010 Graz, Austria. ³Institute of Medical Engineering, Graz University of Technology, 8010 Graz, Austria. ⁴Division of Gastroenterology and Hepatology, Department of Internal Medicine, Medical University of Graz, 8036 Graz, Austria.

*To whom correspondence should be addressed. E-mail: rudolf.zechner@uni-graz.at (R.Z.); gerald.hoefler@medunigraz.at (G.H.)

either *Atgl* or *Hsl*. Cachexia was induced in wild-type C57BL/6 (WT) mice, *Atgl*-deficient (*Atgl*^{-/-}) mice (20), and *Hsl*-deficient (*Hsl*^{-/-}) mice (21) by subcutaneous injection of Lewis lung carcinoma (LLC) cells (22) or B16 melanoma cells (23). Tumor growth was observed in 100% of treated animals. Tumor weights tended to be lower in nonfasted (Fig. 1, A to C) and overnight (o/n)-fasted (fig. S1, A and B) (24) *Atgl*^{-/-} and *Hsl*^{-/-} mice than in WT mice. However, none of the differences reached statistical significance.

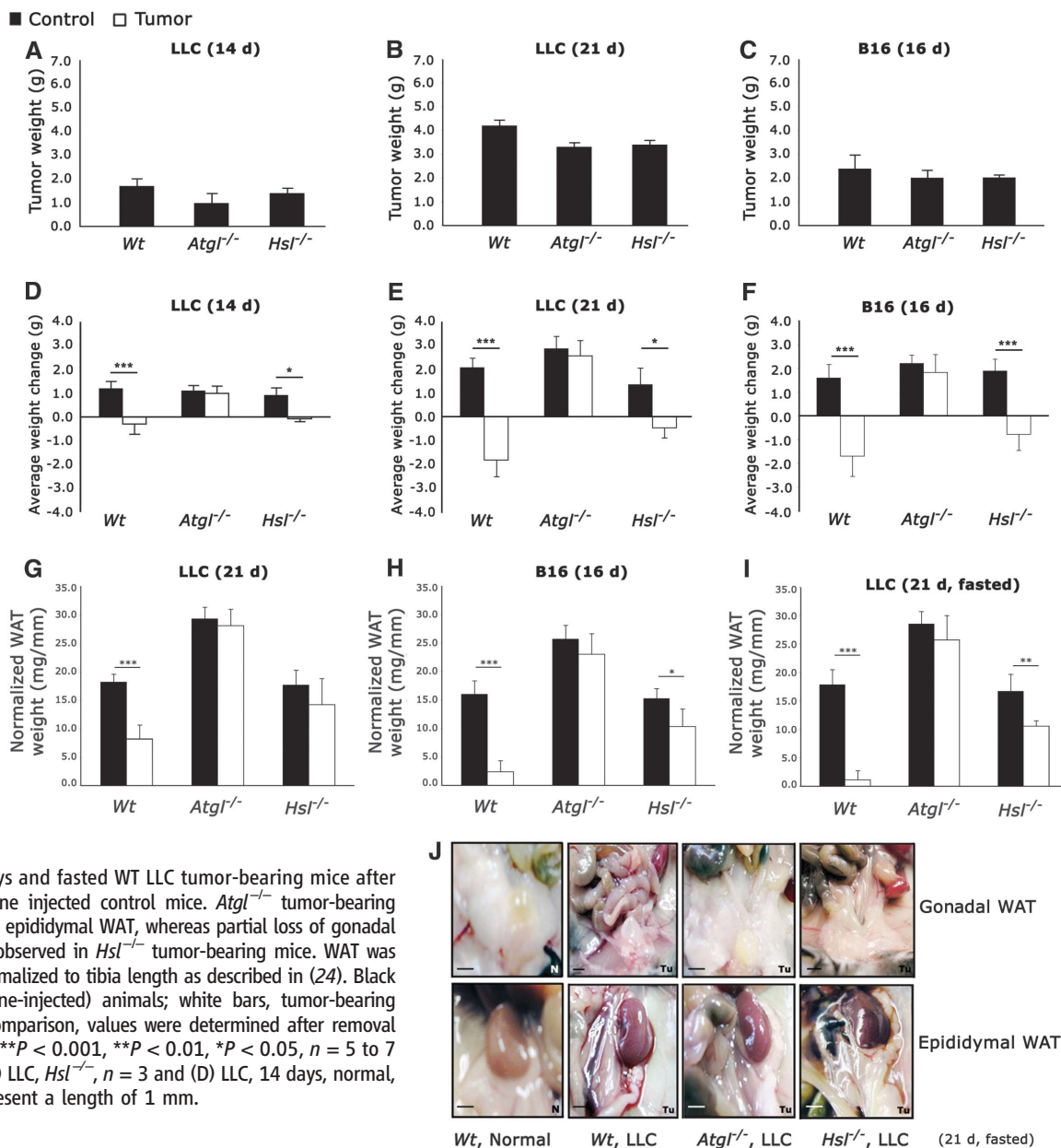
Next we analyzed body weight, plasma metabolite concentrations, and fat mass in mice of all genotypes with or without tumors. Because all of these parameters strongly depend on the feeding status of the mice and to account for any nutritional bias, they were determined in nonfasted and o/n-fasted animals. Total body weight (after subtraction of tumor weight) differed dras-

tically in lipase-deficient mouse models compared with WT mice in response to LLC and B16 (Fig. 1, D to F). Whereas non-tumor-bearing WT mice on normal chow diet gained weight over a period of 3 weeks, WT mice with LLC started to lose weight 14 days after tumor injection, resulting in an average weight loss of 1.8 g after 21 days. In contrast, body weight in *Atgl*^{-/-} mice with LLC was identical to *Atgl*^{-/-} without tumors at all times. *Hsl*^{-/-} mice exhibited an intermediate phenotype. Compared to non-tumor-bearing *Hsl*^{-/-} mice, body weight was reduced. However, the loss was less extreme than in WT mice carrying the tumor. Similar results were obtained in B16-treated mice (Fig. 1 F). Compared with WT mice without tumors, B16-treated mice weighed 3.3 g less 16 days after tumor injection. In contrast, B16-treated *Atgl*^{-/-} mice maintained weights similar to those of untreated *Atgl*^{-/-} mice. *Hsl*^{-/-} ani-

mals were less protected than *Atgl*^{-/-} mice and lost on average 2.7 g of body weight. The differences were even more pronounced in o/n-fasted mice, a condition when lipolysis is physiologically induced (fig. S2). Whereas WT mice with LLC weighed 2.1 g (after 14 days) and 5.5 g (after 21 days) less than WT mice without tumors, *Atgl*^{-/-} mice were totally resistant to weight loss and *Hsl*^{-/-} animals reached intermediate values. Differences in weight loss in response to the tumors were not explained by variable food intake (fig. S3, A and B), because it was similar in all animals during the initial phase of the experiment and decreased uniformly in all tumor-carrying mice during the final 2 to 4 days. Thus, in the mouse, protection from CAC-associated weight loss can be entirely conferred by the lack of ATGL and partially by the absence of HSL.

Fig. 1. Ablation of *Atgl*

protects mice from cancer-associated weight loss and cancer-associated loss of adipose tissue. (A to C) Tumor weights 14 days (d) and 21 days after injecting LLC and 16 days after injecting B16 melanoma (B16) cells were slightly lower in lipase-deficient mice compared with WT. (D to F) WT mice significantly lost weight with tumor progression after injection of LLC and B16 tumor cells, whereas *Atgl*^{-/-} animals did not develop cachexia. *Hsl*^{-/-} mice also lost weight but less than WT mice did. (G) Normalized gonadal and epididymal WAT was reduced by about 55% in nonfasted tumor-bearing WT mice 21 days after LLC tumor implantation, whereas lipase-deficient mice were protected from WAT loss. (H to J) No or minimal gonadal and epididymal WAT was detected upon dissection of nonfasted WT B16 tumor-bearing mice after 16 days and fasted WT LLC tumor-bearing mice after 21 days compared to saline injected control mice. *Atgl*^{-/-} tumor-bearing mice retained gonadal and epididymal WAT, whereas partial loss of gonadal and epididymal WAT was observed in *Hsl*^{-/-} tumor-bearing mice. WAT was dissected, and its mass normalized to tibia length as described in (24). Black bars indicate control (saline-injected) animals; white bars, tumor-bearing animals. To allow direct comparison, values were determined after removal of the respective tumor. ****P* < 0.001, ***P* < 0.01, **P* < 0.05, *n* = 5 to 7 except for (A) to (E) and (G) LLC, *Hsl*^{-/-}, *n* = 3 and (D) LLC, 14 days, normal, *n* = 2. (J) Scale bars represent a length of 1 mm.



Consistent with our previous findings (20, 21), plasma glucose, FA, and TG levels were reduced in o/n-fasted *Atgl*^{-/-} versus WT mice (figs. S4 to S6). In o/n-fasted *Hsl*^{-/-} mice, FA and TG levels were also reduced (although less than in *Atgl*^{-/-} mice), whereas plasma glucose concentrations were unchanged compared with those of WT mice (figs. S4 to S6). The presence of LLC for 14 days did not affect plasma glucose levels in o/n-fasted mice of any genotype (fig. S4A). After 21 days, plasma glucose levels were decreased in tumor-bearing, o/n-fasted WT (-43.2%) and *Hsl*^{-/-} mice (-27.3%) but remained unchanged in *Atgl*^{-/-}

mice when compared to mice of the same genotype without tumors (fig. S4B). These differences in glucose levels in LLC-treated WT and *Hsl*^{-/-} mice were not observed in nonfasted animals (fig. S4C). Similarly, plasma glucose and FA levels of nonfasted B16-treated mice matched those in untreated animals (fig. S4D). Presence of LLC caused an increase in FA levels in WT (fasted: +24.0% at 14 days and +9.9% at 21 days; nonfasted: +54.5% at 21 days) and *Hsl*^{-/-} mice (fasted: +23.4% at 14 days and +25.0% at 21 days) (fig. S5). In contrast, FA levels in tumor-bearing *Atgl*^{-/-} mice remained unchanged compared with those

of *Atgl*^{-/-} mice without tumors independent of the feeding status. Increased FA levels were also observed in nonfasted B16-tumor-bearing WT mice (+27%) (fig. S5D). Serum TG levels were not significantly different in o/n-fasted animals with or without tumors (fig. S6).

To assess the contribution of adipose tissue loss to the tumor-induced weight loss, we determined white adipose tissue (WAT) mass by visual inspection, weighing of surgically removed adipose depots (gonadal and epididymal adipose tissue), and in vivo nuclear magnetic resonance (NMR) WAT quantitation. In nonfasted

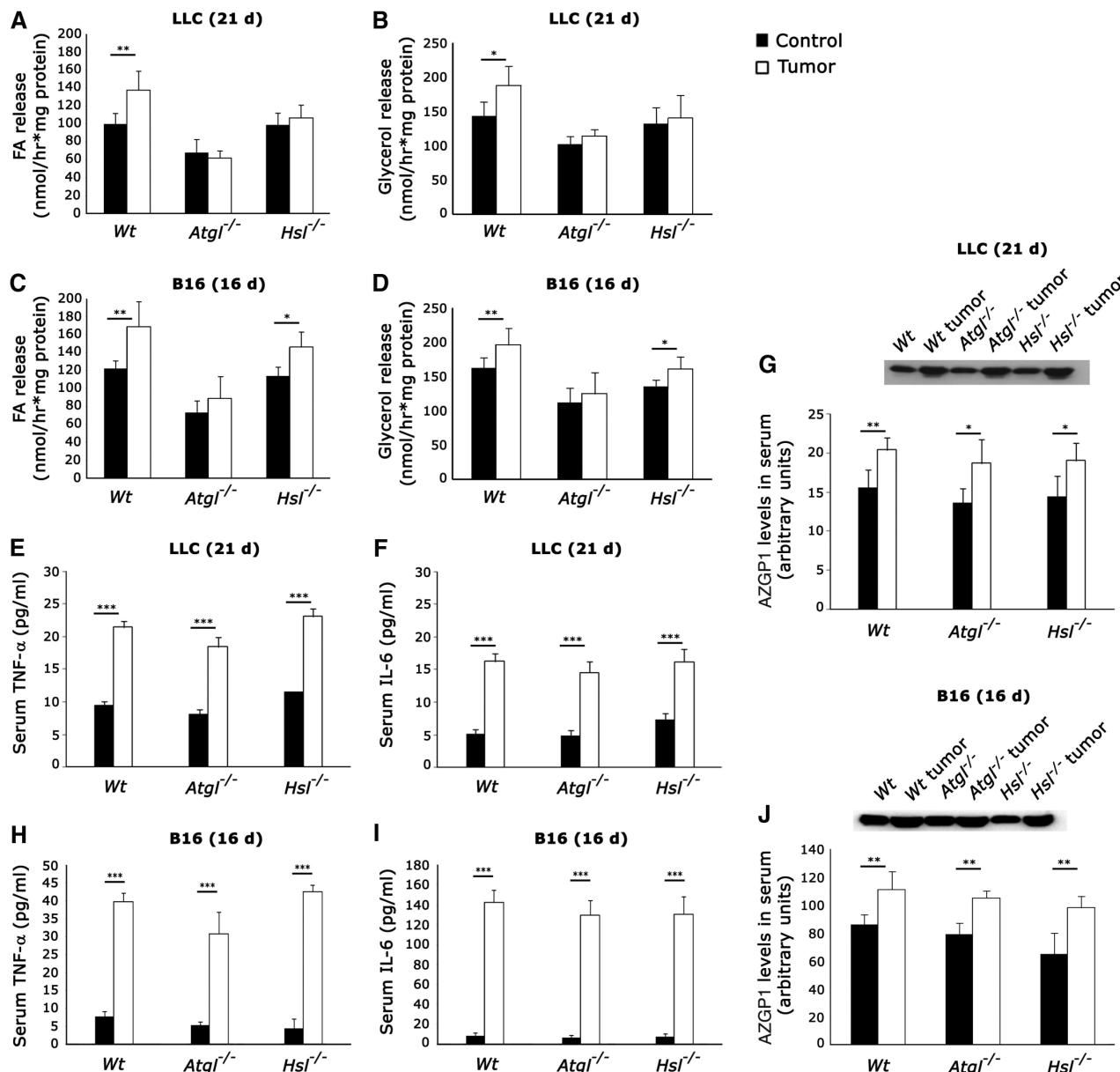


Fig. 2. Loss of WAT in tumor-bearing animals is mainly attributable to lipolysis. Both LLC and B16 tumors significantly increased FAs (A and C) and glycerol (B and D) release from WAT explants in nonfasted tumor-bearing WT mice. LLC-bearing lipase-deficient mice did not exhibit increased FA or glycerol release from WAT explants, whereas increased FA and glycerol release was observed from WAT explants of B16-tumor-bearing *Hsl*^{-/-} mice.

WAT explants from B16-tumor-bearing *Atgl*^{-/-} mice did not show increased FA or glycerol release. (E to J) Lipolytic agonists (TNF- α , IL-6, and AZGP1) were increased in both LLC- and B16-tumor-bearing mice from all genotypes. Black bars indicate control (saline-injected) animals; white bars, tumor-bearing animals. ****P* < 0.001, ***P* < 0.01, **P* < 0.05, *n* = 7 except for (A) and (B), *n* = 3 to 5.

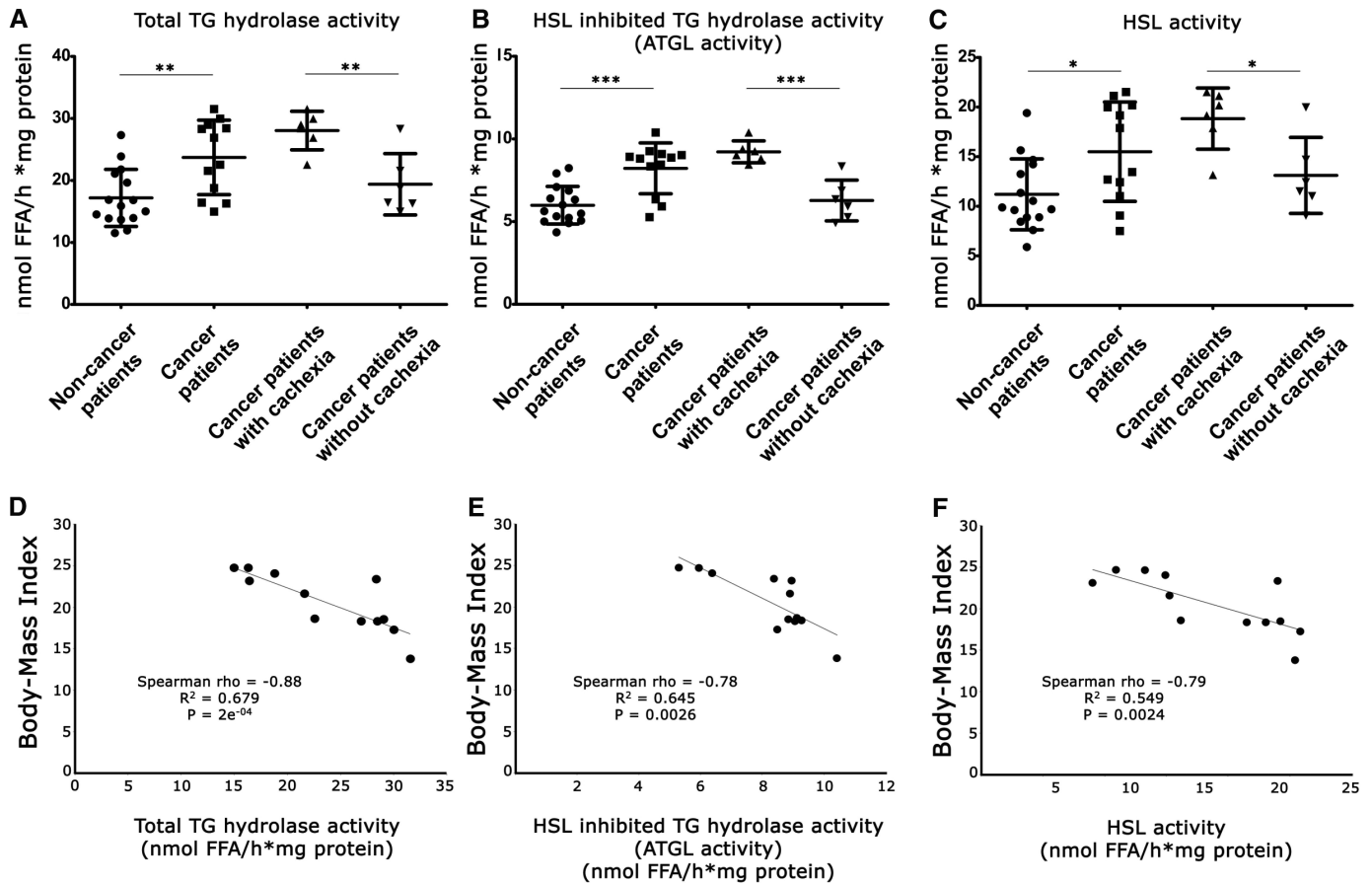
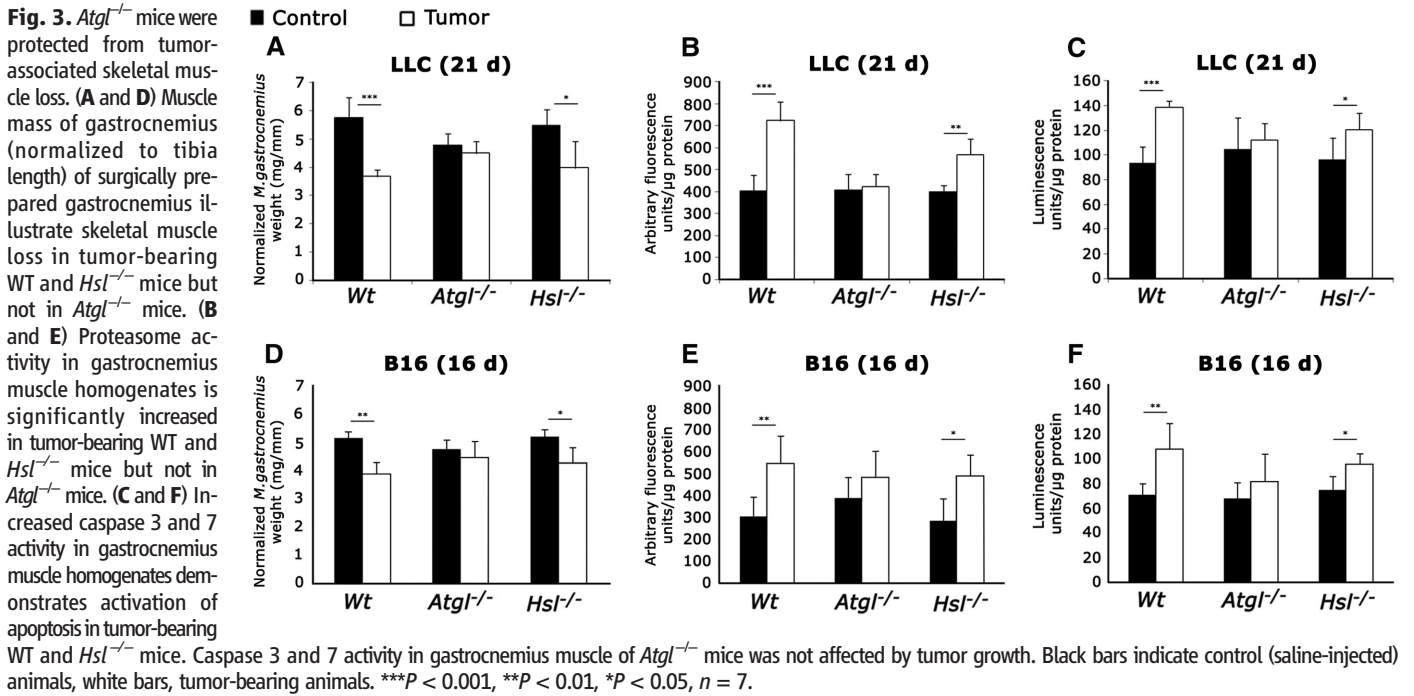


Fig. 4. CAC patients show increased TG hydrolase activity compared with noncachectic patients. Total lipase activity (A), specifically inhibited (HSL, 76-0079) lipase activity (mainly ATGL activity) (B), and HSL activity (determined by subtraction of HSL-inhibited lipase activity from total lipase activity) (C) in visceral WAT of cancer patients compared with those of noncancer patients. Lipase activities in WAT of cachectic cancer patients are significantly higher than in noncachectic cancer patients. Ranges indicate mean \pm standard deviation. (D to F) Total, HSL-inhibited, and HSL lipase activities show negative correlation with BMI of cancer patients. FFA, free fatty acid.

LLC-bearing WT mice, WAT weight decreased by 55% after 21 days of tumor growth (Fig. 1G), which corresponded to a loss of 1.7 g of WAT in NMR analysis (fig. S7A). Nonfasted B16-bearing WT mice lost 85% of WAT weight after 16 days of tumor growth (Fig. 1H) (−2.0 g of adipose tissue mass in NMR analysis, fig. S7B). In contrast, none of the tumors affected WAT mass of *Atgl*^{−/−} mice. In fact, weight of body fat depots and total body fat was increased in *Atgl*^{−/−} mice independent of the presence or absence of tumors when compared to non-tumor-bearing WT mice (Fig. 1, G and H, and fig. S7). This confirms our earlier observation that *Atgl* deficiency causes obesity in mice kept on a normal chow diet (20) and shows that WAT mass is independent of the presence of the tumor. In nonfasted *Hsl*^{−/−} mice, LLC did not affect the weight of WAT depots. However, NMR analyses revealed a total WAT reduction by 0.7 g in (Fig. 1G and fig. S7A). B16 in *Hsl*^{−/−} mice caused a 32% reduction of adipose tissue weight and a 0.9 g WAT loss in NMR analysis (Fig. 1H and fig. S7B). In o/n-fasted animals, the differences were even more striking (Fig. 1, I and J, and fig. S7C). After 21 days, LLC tumors caused the loss of more than 95% of WAT weight (2 g in NMR analysis) in WT mice, whereas adipose mass was again completely retained in LLC-treated *Atgl*^{−/−} mice. *Hsl*^{−/−} mice exhibited an intermediate loss of 37% of WAT weight. Results for LLC-bearing animals were substantiated by magnetic resonance imaging analysis. Taken together, these results show that, independently of feeding status and tumor type, ATGL deficiency completely and HSL deficiency partially protects mice from the loss of WAT.

Tumor-associated loss of adipose tissue in animal models has been mostly attributed to an increase in WAT lipolysis (10–16). Consistent with these reports, the release of FAs and glycerol from WAT explants was increased in WT mice with LLC (38% and 31%, respectively) and B16 (39% and 21%, respectively) compared with mice without tumors (Fig. 2, A to D). This increase in lipolysis did not occur in LLC- or B16-tumor-bearing *Atgl*^{−/−} mice. WAT lipolysis was also attenuated in tumor-bearing *Hsl*^{−/−} mice. Whereas FA and glycerol release from WAT was similar in *Hsl*^{−/−} mice with or without LLC, B16 melanoma formation caused 28% and 19% increases, respectively. To investigate whether changes in TG hydrolase activities underlie the observed differences in lipolytic rates, we measured ATGL and HSL enzyme activities in WAT in response to tumor growth (fig. S8). LLC in o/n-fasted WT mice caused a twofold increase in total lipase activity because of increased ATGL and HSL activity. No tumor-induced increase in WAT lipase activity was observed in *Atgl*^{−/−} mice, whereas in *Hsl*^{−/−} mice total TG lipase activity increased by 2.1-fold because of increased ATGL activity. Thus, LLC and B16 cause an induction of WAT TG hydrolase activity, leading to an increased release of FAs and glycerol from WAT.

This induction of lipolysis is not observed in the absence of ATGL and significantly reduced in the absence of HSL. Thus, lipase deficiency blocks tumor-induced WAT loss.

Several reports have shown that the induction of lipolysis during CAC is mediated by inflammatory cytokines (17), AZGP1 (also designated lipid mobilizing factor, LMF) (18), or cytotoxin-induced death executor proteins (CIDE), such as CIDE-A (25). To investigate whether these lipolytic agonists are increased in cachexia models lacking specific lipases, we assessed their plasma levels. In response to LLC, TNF- α and IL-6 levels were increased (between 2- to 3.2-fold) in all genotypes (Fig. 2, E and F). Similarly, quantitative Western blot analysis revealed that plasma AZGP1 levels were higher in LLC-bearing animals of all genotypes (Fig. 2G). In response to B16, the induction of cytokine release was even more pronounced (Fig. 2, H and I). Plasma levels of TNF- α and IL-6 increased about five- to ninefold and 18- to 21-fold, respectively. Plasma AZGP1 levels were also consistently higher in B16-treated mice of all genotypes compared with untreated mice (Fig. 2J). This suggests that in WT mice the increased concentration of inflammatory and lipolytic agonists induce lipolysis via ATGL and HSL leading to the uncontrolled loss of WAT and cachexia. In the absence of lipases, particularly in the absence of ATGL, this process is disrupted and WAT is retained.

In cancer patients, CAC not only emaciates adipose tissue but also consumes skeletal muscle and cardiac muscle (9, 22, 26, 27). Similarly, we observed that LLC and B16 melanoma in mice lowers skeletal muscle mass and heart weight. Surgically removed gastrocnemius muscle of WT mice injected with LLC (21 days) and B-16 (16 days) weighed 36% and 25% less than that of WT mice, respectively (Fig. 3, A and D), suggesting that muscle loss was less pronounced than the loss of adipose mass. Remarkably, *Atgl*^{−/−} mice suffered no significant loss of gastrocnemius muscle weight in response to the tumors (Fig. 3, A and D). Similarly as in WT mice, LLC and B16 in *Hsl*^{−/−} mice diminished gastrocnemius muscle weight (Fig. 3, A and D), albeit to a lesser degree (−27% and −18%, respectively). Wasting of gastrocnemius muscle was also reflected by a reduction of total muscle protein in WT (−36%) and *Hsl*^{−/−} mice (−22%) in response to B16, whereas *Atgl*^{−/−} mice with B16 melanoma were resistant to the loss of muscle protein (fig. S9). The weight of soleus muscle also decreased in LLC-injected WT mice after 21 days (33%, not statistically significant) and B16-injected WT mice (−27%) (fig. S10). Both LLC and B16 caused a moderate decrease in heart weight (−7.4% and −9.9%, respectively) and total cardiac protein content (−20.1% and −24.9%, respectively) in WT mice but not in *Atgl*^{−/−} or *Hsl*^{−/−} mice (fig. S11). Consistent with our previous observations (20), *Atgl*^{−/−} mice exhibited a twofold increased TG content in gastrocnemius muscle and a 12- to

15-fold increased TG content in cardiac muscle (fig. S12) compared with WT animals.

Muscle atrophy may originate from a decrease in protein synthesis (28) or an increase in protein degradation (9, 22). Studies in a number of experimental models of cachexia suggest that both processes occur simultaneously (9). Animal models of cancer cachexia as well as studies in cancer patients provided evidence that the ubiquitin-proteasome pathway mainly degrades myofibrillar proteins, particularly at later stages of cachexia when patients lost more than 10% of their body weight (29). Additionally, apoptotic cell death characterized by increased activity of caspases contributes to the loss of gastrocnemius muscle in mice bearing the cachexia-inducing MAC16 tumor (30). Consistent with these observations, we detected a marked increase in proteasome activity (Fig. 3, B and E) and an increase in caspase 3 and 7 activity (Fig. 3, C and F) in gastrocnemius muscle of WT mice and *Hsl*^{−/−} mice 21 days after LLC injection and 16 days after B16 injection. In contrast, no significant change in proteasome or caspase 3 and 7 activity was observed in gastrocnemius muscle of *Atgl*^{−/−} mice in response to both tumors (Fig. 3, B, C, E, and F). Changes in the weight of gastrocnemius muscle, caspase 3 and 7 activity, and proteasome activity were not observed in WT and *Hsl*^{−/−} mice, 2 weeks after LLC injection (fig. S13), suggesting that loss of WAT precedes the loss of muscle mass, which is consistent with earlier observations (10).

Previous work showed that cachexia is associated with increased FA oxidation in gastrocnemius muscle (9). Our data confirm these findings, showing 1.8- to 2.5-fold increased mRNA expression levels of genes involved in the regulation of cellular FA uptake (*CD36* and fatty acid transport protein 1, *Fatp-1*), FA transport into mitochondria (carnitin palmitoyltransferase-1 β , *Cpt-1 β*), and mitochondrial function (peroxisome proliferator-activated receptor- γ coactivator-1 α , *Pgc-1 α*) in gastrocnemius muscle samples of WT mice with LLC (fig. S14). mRNA levels in muscle samples of *Atgl*^{−/−} mice were not affected in response to LLC. In *Hsl*^{−/−} mice, mRNA levels increased in the presence of the tumor, although to a lesser extent than in WT mice. This suggests that the catabolic state in CAC mobilizes FA from adipose tissue, leading to an energy substrate switch from glucose to FA use in skeletal muscle.

To test whether the activity of metabolic lipases in WAT also associates with CAC in humans, we determined ATGL- and HSL-mediated TG hydrolase activities of visceral WAT from autopsy samples of 27 patients. Twelve of these individuals had been diagnosed with various forms of malignancies (two adenocarcinomas of the lung, two adenocarcinomas of the colon, two ductal adenocarcinomas of the breast, two adenocarcinomas of the prostate, one hepatocellular carcinoma, one clear cell carcinoma of the kidney, one squamous cell carcinoma of the esophagus,

and one malignant germ cell tumor). Six out of the 12 patients were designated as cachectic according to the definition of Evans *et al.* (31). Total lipase, ATGL, and HSL activities were significantly higher in visceral WAT of cancer patients compared with individuals without cancer and significantly higher in cancer patients with cachexia compared with cancer patients without cachexia (Fig. 4, A to C). Lipase activities in cancer patients without cachexia were similar to those of noncancer patients. A significant inverse correlation was found between total lipase, ATGL, and HSL activities in WAT of cancer patients and their body mass index (BMI) (Fig. 4, D to F). In contrast, lipolytic activities in WAT of noncancer patients showed no correlation with their BMI (fig. S15). Thus, our study provides compelling evidence that the previously observed increase in FA and glycerol release from WAT of patients with CAC (9, 10) is due to up-regulation of ATGL and HSL activities and that increased lipase activities strongly correlate with cachexia.

In summary, our data are consistent with the view that lipolysis plays an instrumental role in the pathogenesis of CAC. The increased catabolism of adipose lipid stores leads to the complete loss of WAT followed by a reduction in muscle mass. The absence of ATGL and, to a lesser degree, HSL reduces FA mobilization, retains WAT and muscle mass, and prevents CAC. Whether the protection of adipose and muscle loss in lipase-deficient mice is a consequence of defective tissue autonomous lipolysis or due to endo-

crine signaling from the tumor or WAT remains to be elucidated. However, pharmacological inhibition of lipases may represent a powerful strategy to avoid the devastating condition of cachexia in response to cancer or other chronic diseases.

References and Notes

- M. J. Tisdale, *Nat. Rev. Cancer* **2**, 862 (2002).
- J. E. Morley, D. R. Thomas, M. M. Wilson, *Am. J. Clin. Nutr.* **83**, 735 (2006).
- W. D. Dewys *et al.*, *Am. J. Med.* **69**, 491 (1980).
- C. Deans, S. J. Wigmore, *Curr. Opin. Clin. Nutr. Metab. Care* **8**, 265 (2005).
- K. C. Fearon, A. G. Moses, *Int. J. Cardiol.* **85**, 73 (2002).
- M. Fouladi *et al.*, *Cancer* **103**, 2189 (2005).
- K. C. Fearon, *Proc. Nutr. Soc.* **51**, 251 (1992).
- M. Lainscak, G. S. Filippatos, M. Gheorghiadu, G. C. Fonarow, S. D. Anker, *Am. J. Cardiol.* **101**, 8E (2008).
- M. J. Tisdale, *Physiol. Rev.* **89**, 381 (2009).
- T. Agustsson *et al.*, *Cancer Res.* **67**, 5531 (2007).
- A. Hyltander, P. Daneryd, R. Sandström, U. Körner, K. Lundholm, *Eur. J. Cancer* **36**, 330 (2000).
- S. Klein, R. R. Wolfe, *J. Clin. Invest.* **86**, 1403 (1990).
- A. Legaspi, M. Jeevanandam, H. F. Starnes Jr., M. F. Brennan, *Metabolism* **36**, 958 (1987).
- M. Rydén *et al.*, *Cancer* **113**, 1695 (2008).
- J. H. Shaw, R. R. Wolfe, *Ann. Surg.* **205**, 368 (1987).
- M. Jeevanandam, G. D. Horowitz, S. F. Lowry, M. F. Brennan, *Metabolism* **35**, 304 (1986).
- J. M. Argilés, S. Busquets, M. Toledo, F. J. López-Soriano, *Curr. Opin. Support. Palliat. Care* **3**, 263 (2009).
- C. Bing *et al.*, *Proc. Natl. Acad. Sci. U.S.A.* **101**, 2500 (2004).
- R. Zechner, P. C. Kienesberger, G. Haemmerle, R. Zimmermann, A. Lass, *J. Lipid Res.* **50**, 3 (2009).
- G. Haemmerle *et al.*, *Science* **312**, 734 (2006).
- G. Haemmerle *et al.*, *J. Biol. Chem.* **277**, 4806 (2002).
- M. van Royen *et al.*, *Biochem. Biophys. Res. Commun.* **270**, 533 (2000).
- I. Kawamura *et al.*, *Anticancer Res.* **19**, 341 (1999).
- Materials and methods are available as supporting material on Science Online.
- J. Laurencikiene *et al.*, *Cancer Res.* **68**, 9247 (2008).
- X. Zhou *et al.*, *Cell* **142**, 531 (2010).
- S. Busquets *et al.*, *Clin. Nutr.* **26**, 239 (2007).
- M. J. Rennie *et al.*, *Clin. Physiol.* **3**, 387 (1983).
- J. Khal, A. V. Hine, K. C. Fearon, C. H. Dejong, M. J. Tisdale, *Int. J. Biochem. Cell Biol.* **37**, 2196 (2005).
- J. E. Belizario, M. J. Lorite, M. J. Tisdale, *Br. J. Cancer* **84**, 1135 (2001).
- W. J. Evans *et al.*, *Clin. Nutr.* **27**, 793 (2008).

Acknowledgments: We thank E. Zechner and C. Schober-Trummler for reviewing the manuscript. The research was supported by the doctoral program Molecular Medicine of the Medical University of Graz (S.D.); GOLD, Genomics of Lipid-Associated Disorders as part of the Austrian Genome Project GEN-AU funded by Forschungsförderungsgesellschaft and Bundesministerium für Wissenschaft und Forschung (Ru.Ze.); SFB LIPOTOX grant no. F30 (Ru.Ze., G.H.), the Wittgenstein Award 2007 grant no. Z136 funded by the Austrian Fonds zur Förderung der Wissenschaftlichen Forschung (Ru.Ze.). S.K.D., Ro.Zi., G.H., and Ru.Ze. hold a patent related to the modulation of ATGL for prevention and treatment of cachexia.

Supporting Online Material

www.sciencemag.org/cgi/content/full/science.1198973/DC1
Materials and Methods
Figs. S1 to S15
References

12 October 2010; accepted 27 May 2011
Published online 16 June 2011;
10.1126/science.1198973

A Pericyte Origin of Spinal Cord Scar Tissue

Christian Göritz,¹ David O. Dias,¹ Nikolay Tomilin,² Mariano Barbacid,³ Oleg Shupliakov,² Jonas Frisén^{1*}

There is limited regeneration of lost tissue after central nervous system injury, and the lesion is sealed with a scar. The role of the scar, which often is referred to as the glial scar because of its abundance of astrocytes, is complex and has been discussed for more than a century. Here we show that a specific pericyte subtype gives rise to scar-forming stromal cells, which outnumber astrocytes, in the injured spinal cord. Blocking the generation of progeny by this pericyte subtype results in failure to seal the injured tissue. The formation of connective tissue is common to many injuries and pathologies, and here we demonstrate a cellular origin of fibrosis.

Most studies on the scar tissue that forms at injuries in the central nervous system (CNS) have focused on astrocytes, and it is often referred to as the glial scar (1–5).

¹Department of Cell and Molecular Biology, Karolinska Institute, SE-171 77 Stockholm, Sweden. ²Department of Neuroscience, Karolinska Institute, SE-171 77 Stockholm, Sweden. ³Molecular Oncology Programme, Centro Nacional de Investigaciones Oncológicas, 28029 Madrid, Spain.

*To whom correspondence should be addressed. E-mail: jonas.frisen@ki.se

There is also a connective tissue or stromal, non-glial, component of the scar (6–10), but it has received much less attention. The generation of connective tissue, with large numbers of fibroblasts depositing extracellular matrix (ECM) proteins, is a general feature of scarring and fibrosis in all organs and in diverse types of pathology (11). In spite of being a major clinical problem that has been extensively studied, the origin of scar-forming fibroblasts has been difficult to establish. Most studies have suggested that they may derive from

circulating cells, proliferating resident fibroblasts, endothelial cells, or epithelial cells (12–14). There are also data indicating that pericytes, perivascular cells wrapping the endothelial cells of capillaries, may differentiate into collagen-producing cells in models of dermal scarring and in kidney fibrosis (15–17).

We have explored the role of pericytes in scar formation after spinal cord injury. We found that *Glast-CreER* transgenic mice (18) enabled recombination of the *R26R-yellow fluorescent protein (R26R-YFP)* reporter allele (19) in a subset of pericytes lining blood vessels in the spinal cord parenchyma, which allowed us to stably and heritably label these cells (20) (Fig. 1 and figs. S1 to S5). The recombined cells had the typical ultrastructural features of pericytes (21), including being encased in the vascular basal lamina, which separates them from endothelial cells and astrocytes (Fig. 1, A to D). The recombined cells represent a distinct pericyte subpopulation that constitutes ~10% of all pericytes in the adult spinal cord [assessed by electron microscopy (EM)]. At positions where processes intersect, the *Glast-CreER*-expressing pericytes were invariably located abnormally to the other pericyte subtype (Fig. 1A and fig. S6). We refer to the pericyte subclass that is recombined in *Glast-CreER* mice as type A pericytes and the other